




An Investigation of the Properties of 3D Printing Materials According to Additive Manufacturing Conditions Using Ultrasonic Wave

Junpil Park¹ · Sunho Choi² · Seoung ho Baek³ · Sang hu Park³ · Yu-Hsi Huang⁴ · Jaesun Lee⁵ 

Received: 2 November 2021 / Revised: 8 March 2023 / Accepted: 9 March 2023 / Published online: 30 March 2023
© The Author(s), under exclusive licence to Korean Society for Precision Engineering 2023

Abstract

3-Dimension (3D) printers are increasingly being used in high-tech industrial applications technology, because they can produce sophisticated products by laminating materials with less time and cost compared to cutting processing, such as conventional machine tools. However, since the reliability evaluation criteria and method for laminated manufacturing products are not clear, accidents cannot be prevented when 3D printed laminates are used as structures and machined parts. In this paper, ultrasonic wave propagation characteristics were evaluated on the specimens manufactured by laminating acrylonitrile butadiene styrene resin materials with a stereo lithography apparatus 3D printer using the ultrasonic inspection method among non-destructive techniques. Specimens were laminated in units of 0.1 mm, and thicknesses of 1, 2, 4, 6 and 8 mm were applied as variables. In addition, the ultrasonic characteristics according to laminating direction were analyzed by laminating diagonally and vertically, including laminating in the horizontal direction, and defect specimens were produced to check whether defects were read. It was found that the ultrasonic velocity of the horizontally laminated specimen having a thickness of less than 4 mm was slower than the ultrasonic reference velocity, and that the ultrasonic velocity was affected according to the laminated direction. In addition, by arranging the defect location of the specimen differently, it was determined whether the defect was detected, and whether it was possible to check the location. Based on the results of this study, it will be possible to broadly apply this technique to advanced industrial technologies through evaluation of the condition and reliability of laminated manufacturing products manufactured with 3D printers.

Keywords Non-destructive testing · Ultrasonic · 3D print · Additive manufacturing product · Wave velocity

1 Introduction

3-Dimension (3D) printer technology began to be commercialized by developing a functional photopolymer system that forms three-dimensionally, beyond the existing two-dimensional printing method by irradiating light on a cross

section and laminating it layer-by-layer. Initially, it was used only in high-tech fields, such as aerospace and automobile industries, but now it has started to be generalized by being distributed to individuals, private companies, and each industrial field. As a result, it is in the spotlight for various high-tech industrial applications, ranging from simple

✉ Jaesun Lee
jaesun@changwon.ac.kr

Junpil Park
junpil@changwon.ac.kr

Sunho Choi
loolysun@changwon.ac.kr

Seoung ho Baek
sky3437@pusan.ac.kr

Sang hu Park
sanghu@pusan.ac.kr

Yu-Hsi Huang
yuhshih@ntu.edu.tw

¹ Extreme Environment Design and Manufacturing Innovation Center, Changwon National University, Changwon 51140, Korea

² Graduate School of Advanced Defense Engineering, Changwon National University, Changwon 51140, Korea

³ School of Mechanical System Design, Pusan National University, Busan 46241, Korea

⁴ Department of Mechanical Engineering, National Taiwan University, Taipei City 10617, Republic of China (Taiwan)

⁵ School of Mechanical Engineering, Changwon National University, Changwon 51140, Korea

prototype mock-up production to medical fields, such as skulls and artificial organs; machinery industries, such as car bodies and internal combustion engine parts; bridges and 3D printing housing construction; and even space rockets and satellites [1–5]. As 3D printers have become more common, production costs and operating and maintenance costs have been reduced, and research is actively underway to improve quality and increase production efficiency [6]. However, for use in various high-tech industries, inspection methods are required to determine the durability of 3D printers and the presence or absence of defects. The 3D printer has the advantage of being able to quickly manufacture products and replace parts needed in the industrial field, because it has small manufacturing process time and cost, and can freely produce shapes that are not allowed in the cutting method using existing machine tools. However, there are disadvantages, in that it is weak in impact strength and vulnerable to heat, because the lamination process technology has not been much developed. In addition, due to low reliability and durability, bending of the output and internal fracture are major problems. Although research on process technology is being actively conducted, due to the characteristics of multi-layer laminates it is difficult to evaluate internal defects and manufacturing completeness. Stereo-lithography apparatus (SLA) and fused deposition modeling (FDM) methods are common in 3D printers, and both processes are manufactured by projecting lasers to cure liquid fuel (Resin) in layers. Although the output speed is fast and has high precision, the production of air gap and strength in the output is reduced due to various variables in the laminating process, such as the precision of the device, and the external environment when laminating liquid fuel. Since defects can be a direct cause of brittle fracture, it is very important to detect and evaluate them in terms of the safety and reliability of 3D print outputs. Although 3D printing is being expanded as temporary replacement parts for various equipment, fatigue failure due to the continuous accumulation of fatigue damage in industrial sites can cause great casualties in the operation stage. In some industrial fields, 3D printers are used to manufacture and operate temporary parts, but the inspection standards are not clear, and reliability problems due to deformation and cracking have been raised [7, 8]. In order to solve these problems, various studies on the safety of 3D printer output have been attempted domestically and internationally.

First, considering the research trends related to 3D printer fabrication and evaluation, S. Park et al. manufactured a tensile test specimen in the SLA method, conducted research on the mechanical characteristics according to the lamination thickness and direction, and confirmed that the tensile strength was higher than the vertical test specimen [9]. P.G. Ikonov designed a skeletal structure model without additional support to use 3D printers in the medical field, and studied 3D printer selection and imitation

design structure methods suitable for actual human bone fabrication using various 3D printers [10]. In addition, various studies have evaluated the strength measurement and output state that change according to various conditions, such as output temperature, internal filling amount, output pattern, and lamination direction [11–13]. Even in the non-destructive field, by grafting the existing non-destructive inspection technique to a 3D printer, research in the field of defect detection and real-time defect detection of laminate manufactured products according to the output method is in progress. P. Lawely conducted defect detection on 3D printer output with ultrasonic C-Scan, and compared it with simulation results [14]. M. Elsaadouny and co-authors used synthetic aperture radar (SAR) to detect defects in polylactic acid (PLA)-type 3D printer output, and also verified the non-destructive test through machine learning and convolution neural network (CNN) learning using the acquired data [15–17]. In addition, many researchers are studying how to improve the surface of 3D printer output using ultrasonic [18–20].

As such, most of the studies evaluated the strength and output state according to the production conditions, such as the output temperature of the 3D printer output, the amount of filling inside, the output pattern, and the direction of lamination [21]. In addition, research on the application of non-destructive testing techniques was conducted only to determine the presence and form of defects [22]. The evaluation of strength and output condition only measures the strength of the product and cannot prevent accidents due to defects occurring during use. There is a study of micro-defect detection due to the layer-by-layer deposition process, such as near-surface and surface defects of a Laser powder deposition monolayer using laser ultrasonic [23]. In addition, there is a lack of research cases that approach ultrasonic non-destructive testing techniques and ultrasonic basic theories or evaluate the ultrasonic propagation characteristics of printed materials in consideration of laminating of multi-layer outputs [24]. Defect detection without considering the ultrasonic propagation characteristics cannot estimate the exact location of the defect. To verify the lamination rate and reliability of the 3D printed output after production is complete, it is necessary to apply a method that can inspect the laminate without destroying it. As an alternative, a non-destructive inspection technique should be applied. There are various inspection methods for the non-destructive technique, and suitable inspection techniques for inspecting laminates include radiographic testing (RT) and ultrasonic testing (UT). Artificial defect geometries produced by metal additive manufacturing are often inspected with RT [25], but due to radiation regulations, RT has many limitations in evaluation and the inspection process takes a long time. That's why UT is a good alternative for inspecting 3D printed output. UT has a variety of techniques for controlling

residual stress and evaluating the initial state and micro-defects of materials [26–31].

This study, rather than focusing on defect detection using ultrasonic waves, compares theoretical and experimental values through the correlation between the thickness of laminated outputs and ultrasonic waves according to the laminating direction using a commonly used SLA 3D printer. Therefore, the ultrasonic wave propagation characteristics according to the lamination thickness and angle of the acrylonitrile butadiene styrene resin (ABS Resin) output of the SLA method 3D printer were studied. Based on the study of ultrasonic propagation characteristics, defects were manufactured inside the specimen, and it was confirmed whether defect detection and defect location could be determined. As a result, a non-destructive evaluation method of 3D printer output using ultrasonic defect detection technique was presented to check the deviation of the ultrasonic propagation velocity, to enable reliable on-site inspection for various defects existing in laminated products.

2 Theory

2.1 Pulse Echo Technique

The ultrasonic wave causes a vibrator to vibrate by any vibration, which is converted into mechanical energy by the piezoelectric effect, and is converted back into electrical energy, which can be confirmed on the oscilloscope.

Ultrasonic waves are classified into longitudinal waves and transverse waves, as particles vibrate parallel to or perpendicular to the direction of wave propagation, respectively. In addition, because the bonding force between particles of each material is different, the velocity of ultrasonic waves varies depending on the propagating medium.

The ultrasonic velocities of the longitudinal and transverse wave are expressed by Eqs. (1) and (2), respectively:

$$C_L = \sqrt{\frac{E}{\rho} \times \frac{1 - \nu}{(1 + \nu)(1 - 2\nu)}} = \sqrt{\frac{K + (4/3)G}{\rho}} \quad (1)$$

$$C_s = \sqrt{\frac{E}{\rho} \times \frac{1}{2(1 + \nu)}} = \frac{\sqrt{G}}{\rho} \quad (2)$$

where, ρ is the density, ν is the Poisson’s ratio, E is the elastic modulus, K is the bulk elastic modulus, and G is the shear modulus.

The ultrasonic waves generated by the probe pass through a couplant (Glycerin) for contact between the probe and the specimen, and then return by passing through the specimen, and reflecting from the bottom of the specimen. The returned ultrasonic wave is converted by

the transducer into an electric pulse. At this time, since the transmission speed of ultrasonic wave is different for each material, in this experiment, the sound speed of ABS resin and acrylic material was inputted, respectively. The wave velocity wave can be calculated if the thickness information of the object and the return time after reflection from the bottom are known. Equation (3) below expresses the velocity of ultrasonic wave:

$$c = \frac{2 \times d}{\Delta t} \quad (3)$$

where, d is the thickness of the specimen, and t is the measurement of the reciprocal travel time of the ultrasonic wave that passes through the specimen, and is reflected back from the bottom.

In this experiment, the pulse–echo method was used among ultrasound techniques. An experiment was conducted to measure the position of a defect and the thickness of an object by injecting an ultrasonic wave into the output of the SLA method 3D printer, and receiving the reflected ultrasonic wave. Figure 1 shows the pulse–echo method. If the thickness d of the specimen is known and the reciprocal travel time t of the ultrasonic wave reflected from the bottom surface is known, the ultrasonic velocity of propagation inside the material can be measured. By measuring the ultrasonic velocity of a 3D printer product having each thickness, it is possible to know the physical ultrasonic velocity that changes according to the layer thickness compared to the ultrasonic velocity that can be physically derived from the raw material in theory.

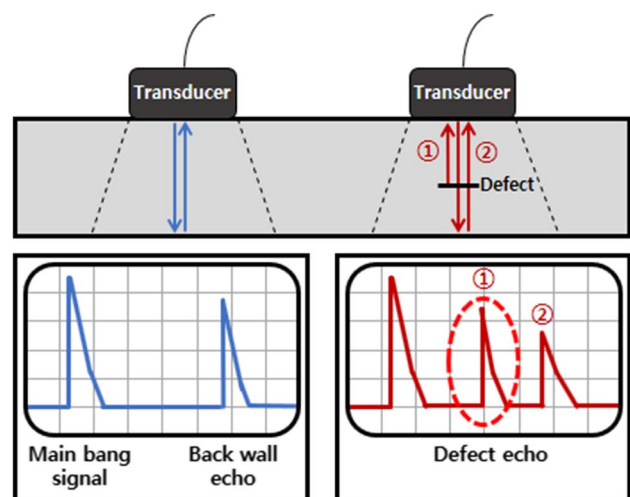


Fig. 1 The principle of Ultrasonic testing pulse–echo

2.2 Ultrasonic Wave Reflection Coefficients that Propagate Vertically Within a Multilayer Structure

Figure 2 shows that when ultrasonic waves pass through a multi-layer structure, the longitudinal wave velocity and acoustic impedance of ultrasonic waves vary, depending on the material properties and the direction of the boundary layer, and there is a difference in the reception time and energy ratio.

When ultrasonic waves passing through one material move to a material with different physical properties, some of the ultrasonic waves are transmitted, and some are reflected at the interface. Therefore, the reflection coefficient, which is the ratio of ultrasonic energy reflected at the interface to the input energy, is calculated.

Equation (4) shows the wave equation for longitudinal wave:

$$\frac{\partial^2 u_x}{\partial x^2} = \frac{1}{c_L^2} \frac{\partial^2 u_x}{\partial t^2} \quad (4)$$

Defining acoustic impedance as $Z = \rho c_L$, reflection and transmission coefficient can thus be written as Eq. (5) [32].

$$R = \frac{Z_2 - Z_1}{Z_1 + Z_2}, T = \frac{2Z_2}{Z_1 + Z_2} \quad (5)$$

Based on the formula derived above, the acoustic impedance and energy ratio reflected from the multi-layer structure can be obtained.

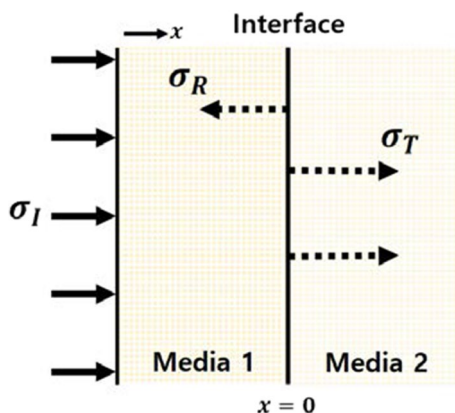


Fig. 2 Ultrasonic waves propagate vertically within the multi-layer structure

3 Experimental Setup and Specimen

3.1 Experimental Setup

In this study, pulse–echo method was used, and Fig. 3 shows a schematic of the experimental set-up. A high-voltage pulser (Ritec's RAM-5000) was used to transmit and receive the pulser echo method, and a (1, 5, 10) MHz single transducer (Olympus) was used to select the optimal frequency. At 1 MHz, the wavelength was longer than that of 5 and 10 MHz, so the specimen was not suitable for use in thin specimens, and it was confirmed that it overlapped with the main bang signal. 10 MHz had good resolution, so reception was good at 1 mm, but at 8 mm, the reception signal was very weak due to signal scattering and attenuation due to the characteristics of the ABS resin material, a polymer composite. Finally, in this study, 5 MHz frequency was selected and the experiment was carried out. Ultrasonic was transmitted and received in 1 cycle to avoid overlapping signals due to thin specimens. In addition, the signal was saved using an oscilloscope (Lecroy's Wave-surfur 3074). Figure 4 shows that the prepared specimens used an acrylic delay line to avoid the main bang signal and interference when detecting the bottom or defects near the surface, and below a certain thickness. Through this, the correlation between the thickness measurement and defect detection of the 3D printer laminated output and the laminating thickness was confirmed.

3.2 Specimen

3.2.1 Intact Specimen with Horizontal Lamination Layer Direction

In this study, an SLA-type 3D printer (UnionTech's Lite600) was used for the experiment, and it was fabricated in a horizontal laminating method, which is generally manufactured. Unlike the FDM method, which generally heats filaments and extrudes and laminates them through a nozzle, SLA is a photocurable resin molding method, and consists of a water tank, laser, and mirror. By reflecting the circular laser with a mirror, heating the resin in the water tank, curing it, and laminating it layer-by-layer to form it, the output time is slow compared to FDM, but the output error and surface roughness show excellent precision. Each specimen was produced by the SLA 3D printer method, and used an ABS resin material (JS-UV-2016-B of Shenzhen Kings 3D Printer Co., Ltd.), which is a liquid photocurable resin. Table 1 shows the main properties of the ABS resin material used in this specimen:

Fig. 3 Experimental setup for 3D printer material by ultrasonic wave

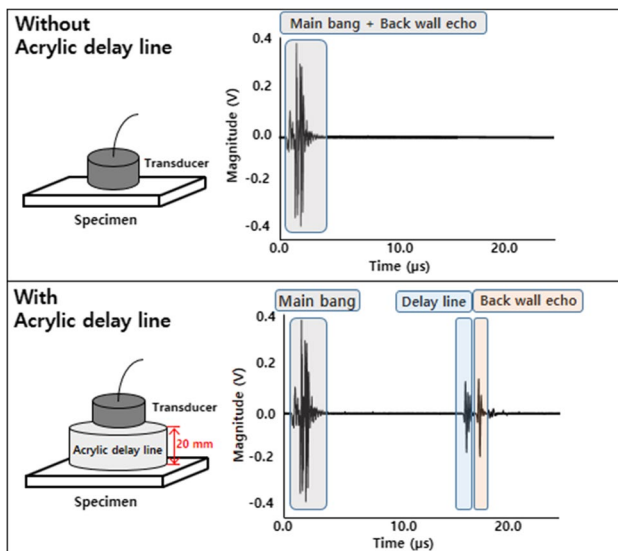
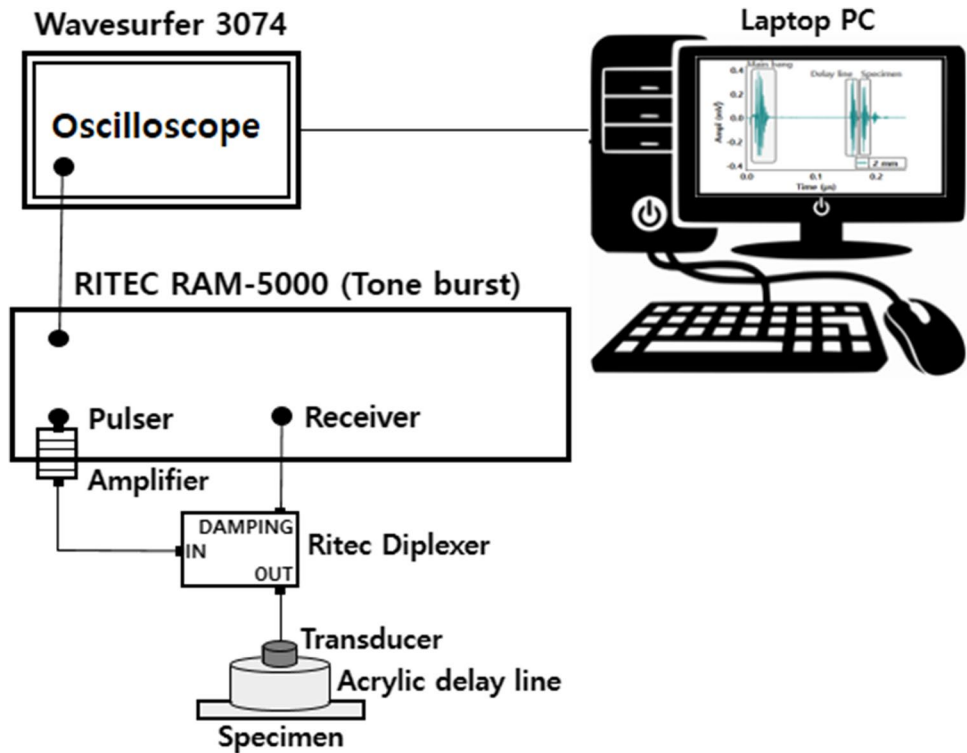


Fig. 4 Comparison of signals with and without delay line

Table 1 Material properties of JS-UV-2016-B

Material	Young’s modulus (MPa)	Poisson’s ratio	Density (g/cm ³)
JS-UV-2016-B	(38–56)	(0.4–0.42)	(1.12–1.18)

Figure 5 shows that a total of 3 sets of specimens were produced to secure reliability of inspection. The intact specimens were used to check the correlation coefficient of the ultrasonic velocity for each layer thickness to check the material properties change according to the layer thickness of the 3D printer. The 50 mm × 50 mm specimens were prepared with different thicknesses of 1, 2, 4, 6, and 8 mm to set the thickness as a variable. When the 3D printer was laminated once, the thickness of the layer was set to 0.1 mm, and the inner filling density was set to 100%, without additional support. At this time, to manufacture each specimen uniformly, 1 set per bed was manufactured.

3.2.2 Intact Specimen with Horizontal Diagonal and Vertical Laminating Directions

To understand the correlation of ultrasonic waves according to the lamination direction, specimens with different lamination directions were manufactured by applying the same material and processing conditions as previously manufactured. The laminating directions were horizontal (0°), diagonal (45°), and vertical (90°), and each of the 3 sets were manufactured according to the direction. The size of the specimen was manufactured as shown in Fig. 5. Figure 6 shows the laminating direction photographed using LV-SEM equipment.

3.2.3 Defects Specimen

The defect specimens are produced by depicting artificial cracks that may occur due to lamination defects, such as pores, and various factors that occur due to problems in the

3D printer process. Their size is difficult to realize in real situations, so they were manufactured as shown in Fig. 7 with the purpose of detecting defects in the output of the SLA 3D printer. The size of each specimen was 150 mm × 150 mm, and the thickness was 8 mm.

Fig. 5 Intact specimen with horizontal lamination layer direction

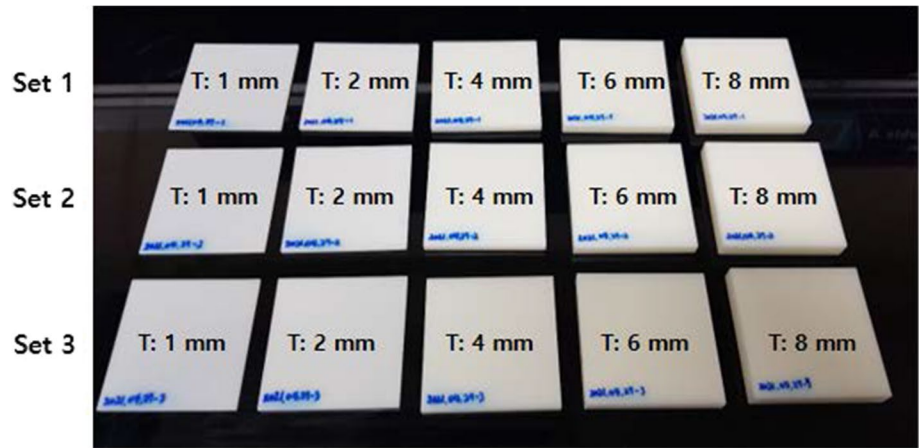


Fig. 6 Intact specimen with laminating direction. **a** Horizontal, **b** Diagonal, **c** Vertical

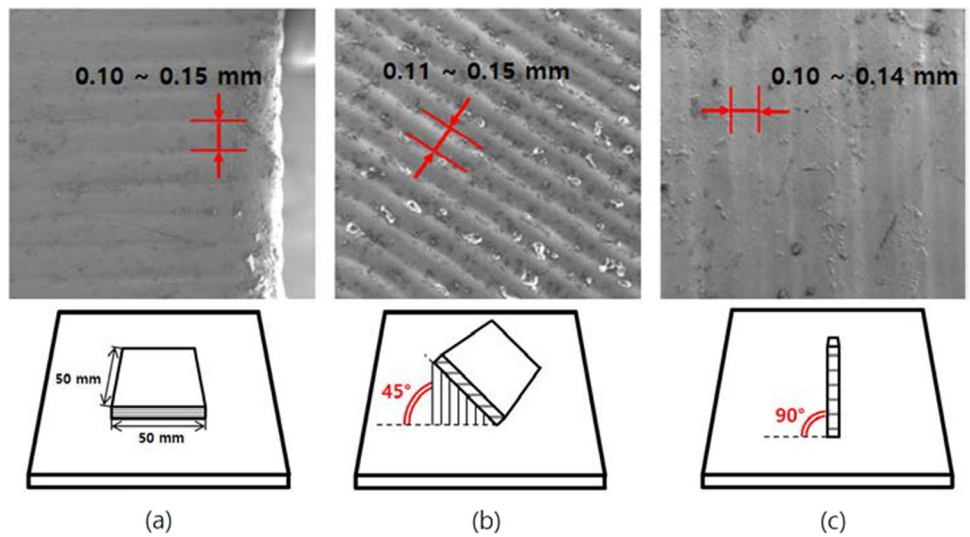
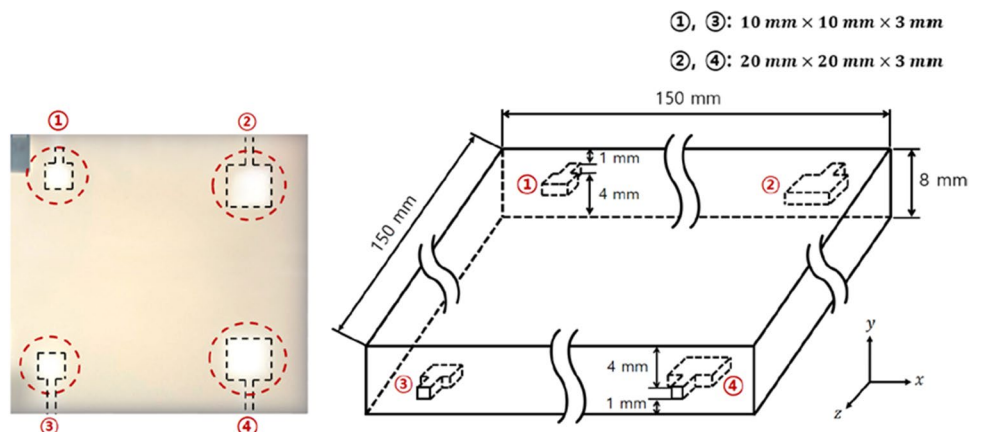


Fig. 7 Defects specimen



Defects were manufactured by emptying four spaces without using additional supporters inside the specimen during the additive manufacturing process, and parts except for defect parts were manufactured by laminating without empty spaces. Figure 7 shows the size and location of the defect. Defects were made at (1 and 4) mm from the surface.

4 Experimental Results

4.1 Experimental Result of Intact Specimen with Horizontal Lamination Layer Direction

The SLA defect specimen with constant lamination conditions to be measured was made of ABS resin material, and at this time, each specimen was subjected to repeated experiments to reduce the standard deviation. Figure 8 shows the ultrasonic measurement results according to the number of laminations, and as can be seen from each result, the first shows the main bang signal, the second shows the signal from the 20 mm acrylic delay line, and the third shows the signal of the specimen manufactured by 3D printer. At this time, the thickness of the specimen can be estimated by considering the pulse interval and the ultrasonic velocity in each medium. Basically, the ultrasonic longitudinal wave velocity in ABS resin is 2,250m/s. Since this study is to investigate the correlation behavior of ultrasonic waves in laminate manufactured products, the magnitude of the amplitude is not meaningful.

Figure 9 shows the results of the experiment of 3 sets of intact specimens laminated in the horizontal direction as a velocity graph. Table 2 shows the error rate compared to the reference wave velocity of ABS Resin. Error rates of 16.72 and 10.65% were generated in specimens of 1 and 2 mm, respectively, and it can be confirmed that the reference ultrasonic velocity and large error values were generated. When the thickness was more than 4 mm, it was close to the average value, and gradually converges to the average value. This

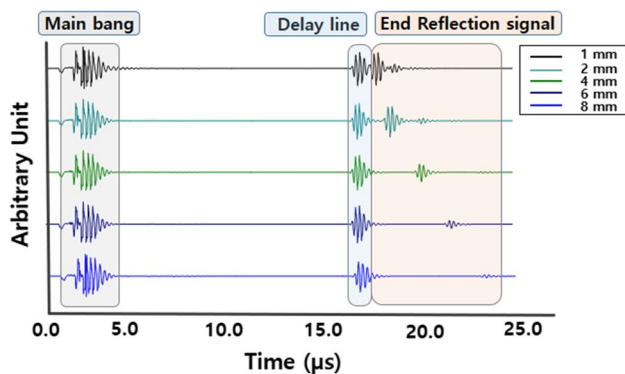


Fig. 8 Experimental result

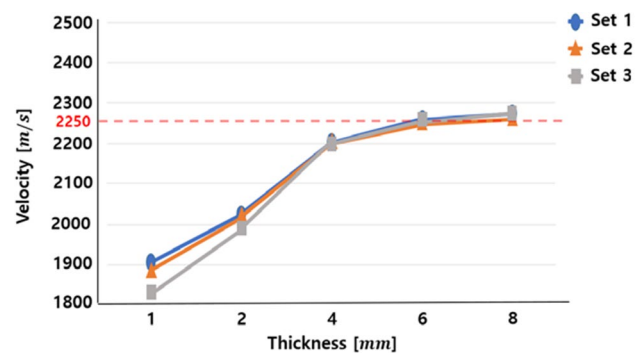


Fig. 9 Wave velocity by thickness

means that the SLA 3D printer laminates 0.1 mm at a time, so it is judged that the change in physical properties or the internal filling amount cannot fill 100%, or if the thickness is thin, deformation occurs in the process of hardening after lamination.

When analyzing the results of the intact specimen, there is no additional signal reflected from the inside of the specimen made of acrylic delay line and ABS resin. This is a very different result from metal, because in the case of ABS resin, since it is a polymer composite, the composition of the material is not completely uniform. In addition, the SLA method was used, which among the actual 3D printer methods is very sophisticated, but looking at the LV-SEM imaging results, in the commercial 3D printer, the thickness of the layer entered into the production program and the actual thickness were not uniform, so there was a slight difference. Also, inclusions and pores were present on the surface or cross-section. The ABS resin material is a composite of acrylonitrile, butadiene, and styrene, and is a heterogeneous material composed of particles with different density and elastic modulus. For these complex reasons, each impedance generates resistance, and the signal emitted by the pulsar is scattered and attenuated, which has a great influence on LV-SEM imaging, as well as ultrasonic testing. When the specimens were laminated once, the thickness was fixed at 0.1 mm, and when the laminated direction was horizontal to the bed, different number of laminates was set as a variable. At less than 4 mm, the ultrasonic wave was slower than the standard wave velocity, and it was confirmed that there was

Table 2 Wave velocity error rate

Thickness (mm)	Velocity (m/s)	Error rate (%)
1	1,874	16.72
2	2,010	10.65
4	2,202	2.11
6	2,256	0.29
8	2,271	0.94

a deviation even with the same thickness. Due to the nature of the SLA 3D printer process, it repeatedly expanded and contracted during the curing process using a high-temperature laser, and could not be laminated consistently. This is thought to be because the inflow of foreign substances, such as dust or micro-pores, affect the mechanical properties of the ABS resin material, which has weak bonding strength. In the case of ≥ 4 mm, it was confirmed that the ultrasonic velocity converges to the average value. These experimental results show that the error in the average lamination thickness confirmed in the LV-SEM results did not significantly affect the ultrasonic experiment. The difference in acoustic impedance is caused by the bonding force between particles according to the laminating direction, and it is judged that the difference in impedance has a greater effect on ultrasonic wave propagation. The lamination angle experimentally proved the ultrasonic basic theory that as the elastic modulus of the material increases, the ultrasonic velocity increases. Tables 3 and 4 show the error range for the laminated materials in the diagonal and vertical directions.

4.2 Experimental Result of Intact Specimen with Horizontal Diagonal and Vertical Laminating Directions

Experiments with specimen with different lamination directions were also tested with the same test set-up as for specimens with the same lamination direction. Figure 10 shows a graph of the velocity and deviation for each thickness of specimen in which the lamination directions are not the same. This result proves that the lamination direction of the 3D printer output affects the mechanical properties. In general, since ultrasonic waves are greatly affected by the bonding force between particles, when the ultrasonic progress time and speed according to the laminating direction were compared, it was confirmed that when the laminating conditions were constant, the ultrasonic progress speed gradually converges within the standard data error range. In addition, in the case of the horizontal laminating direction in the SLA method, it was lower than the standard velocity of 2,250 m/s at less than 4 mm, but converged to the standard velocity at 4 mm or more. However, in a previous study, when the tensile test was conducted with different laminating directions,

Table 3 Wave velocity error rate (Diagonal)

Thickness (mm)	Velocity (m/s)	Error rate (%)
1	1904	15.38
2	2157	4.14
4	2373	5.47
6	2402	6.76
8	2429	7.96

Table 4 Wave velocity error rate (Vertical)

Thickness (mm)	Velocity (m/s)	Error rate (%)
1	2037	9.47
2	2312	2.76
4	2321	3.16
6	2396	6.49
8	2374	5.51

the actual velocity of ultrasonic wave was also different, because the Young's modulus of the material was changed. Based on the above results, it was confirmed that the laminated thickness did not significantly affect the ultrasonic wave, but the number of laminates and the laminating direction had a great influence on the ultrasonic behavior. This can be seen as a difference from the reflection coefficient propagating within the multilayer structure. Therefore, the ultrasonic behavior of the ABS Resin material linearly converges to the ultrasonic standard velocity at the number of times of laminating over a certain level, and if a laminating direction has a certain angle, the standard value is different.

4.3 Experimental Result of Defect Specimens

Based on the results of the intact specimen, a thickness close to the standard data was selected. Artificial defects were processed on a specimen with a thickness of 8 mm, and defects were detected. Defect specimens were laminated horizontally by 0.1 mm in the same laminating direction as the intact specimens. For defects, the amount of filling was 0% at 1 and 4 mm in the depth direction from the upper surface of the specimen, 10 mm \times 10 mm wide and 2 mm thickness. Figure 11 shows the experimental results.

Equation 3 can be used to estimate the position of the defect based on the signal reflected from the defect, and the reflected Δt from defects #1 and #2 are 0.99 μ s and 1.03 μ s. Converting to ultrasonic velocity based on the reflected time yields 2,202 m/s and 2,116 m/s, respectively. In addition, the

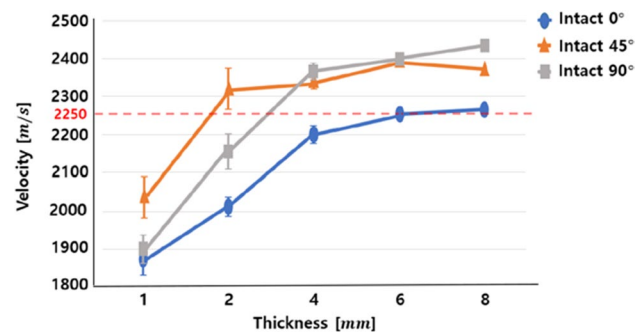


Fig. 10 Wave velocity by thickness

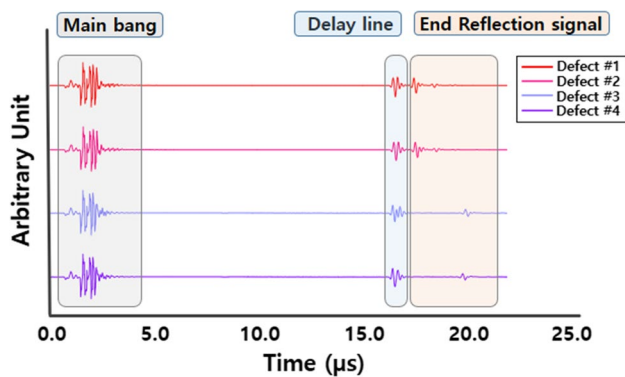


Fig. 11 Experimental result of defect specimen

values of $2,281\text{m/s}$ and $2,222\text{m/s}$ were measured for defects #3 and #4. This becomes a value that cannot be estimated without knowing the thickness of the 3D printer output and the location of the defect. As can be seen from the results of the previous horizontally laminating intact specimen, as it converges to the physical ultrasonic velocity of the raw material at 4 mm or more, accurate data can be extracted only when the Δt of the reflected signal after passing the delay line is $3.45\mu\text{s}$ or more. When the Δt value is less than $3.45\mu\text{s}$, the thickness of the defect can be inference by comparing it with the data measured on the defect specimen as shown in Fig. 12.

5 Conclusion

In this study, ultrasonic-based material characteristics were analyzed according to the lamination manufacturing conditions to verify the reliability of the existing 3D printer product strength and defect measurement techniques.

1. When the laminating direction is horizontal, theoretically, the ultrasonic velocity of the ABS resin material and the experimental results were compared and analyzed. When the laminating direction is horizontal, it can be confirmed that the reference signal is gradually converging at 4 mm or more, and it is confirmed that the ultrasonic velocity is low when the laminating direction is less than 4 mm. It was determined that the internal properties of the thin specimen changed due to heat generated during the lamination process, and the difference from the reflection coefficient propagating in the multilayer structure showed a large error with the actual reference ultrasonic velocity.
2. As a result of experimenting with different laminating directions, it can be confirmed that the velocity of the standard ultrasonic wave is faster than the standard ultrasonic speed. As for this tendency, the error in the average laminating thickness confirmed in the LV-SEM result does not have a significant effect on the ultrasonic experiment, and It can be seen that the coupling force has a greater effect on ultrasonic wave propagation due to the difference in acoustic impedance. Based on this, the basic ultrasonic theory that the lamination angle becomes higher as the elastic modulus of the material increases was experimentally proved.
3. Although the test results of the defect specimen confirmed that the presence or absence of the defect could be determined, it was impossible to accurately target the position because the signal reflected from the delay line was less than $3.45\mu\text{s}$. However, it was possible to estimate the defect value by comparing it with the intact specimen signal.

Through this study, it was confirmed that when manufacturing a 3D printer product, the laminating direction and

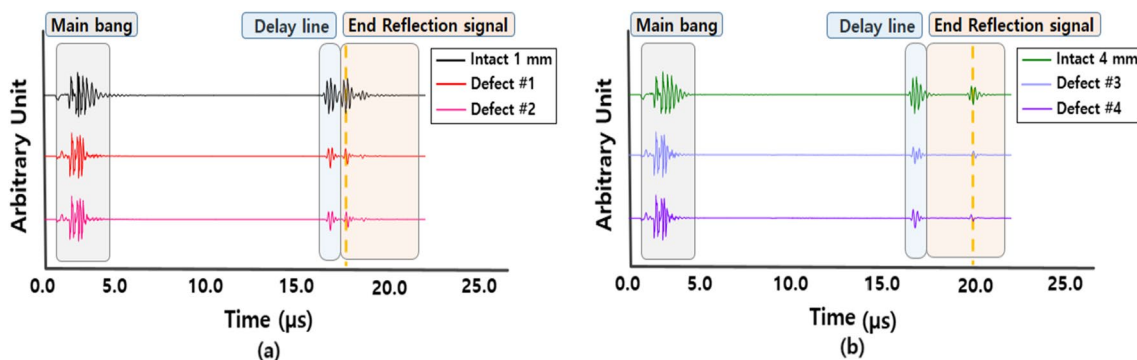


Fig. 12 Comparison of experimental result. **a** Data from intact specimen 1 mm and defects #1 and #2, **b** Data from intact specimen 4 mm and defects #3 and #4

thickness should be considered according to the characteristics of the product to be manufactured. In addition, it was confirmed that the ultrasonic speed, which varies depending on the thickness, needs to be corrected and applied in order to find the exact location of the defect when the defect occurs inside the initial product and during use. In this study, the relationship between the thickness of the output and ultrasonic waves when applying the ultrasonic non-destructive testing to 3D printer products, and presented the reference value of the ultrasonic reflection signal when applying the ultrasonic testing. This will be of great help in terms of product stability by securing reliability and saving time and cost due to damage by manufacturing products applied to major high-tech industrial facilities.

Acknowledgements This work was supported by a National Research Foundation of Korea (NRF) grant, funded by the Korea government (MSIT) (No. 2019R1A5A808320112) and the Ministry of Science and Technology (Republic of China) under Grant MOST 107-2221-E-002-193-MY3.

References

- Ho, C. M. B., Ng, S. H., Li, K. H. H., & Yoon, Y. J. (2015). 3D printed microfluidics for biological applications. *The Royal Society of Chemistry*, 15, 3627. <https://doi.org/10.1039/C5LC00685F>
- Nate, K. A., Hester, J., Isakov, M., Bahr, R., & Tentzeris, M. M. (2015). A fully printed multilayer aperture-coupled patch antenna using hybrid 3D / inkjet additive manufacturing technique. *Proceedings of European 45th Microwave Conference*, 03, 7–10. <https://doi.org/10.1109/EuMC.2015.7345837>
- Otter, W. J., & Lucyszyn, S. (2016). 3-D Printing of microwave components for 21st century applications. *2016 IEEE MTT-S International Microwave Workshop Series on Advanced Materials and Processes for RF and THz Applications*. <https://doi.org/10.1109/IMWS-AMP.2016.7588327>
- Rayna, T., & Striukova, L. (2016). From rapid prototyping to home fabrication: how 3D printing is changing business model innovation. *Technological Forecasting & Social Change*, 102, 214–224. <https://doi.org/10.1016/j.techfore.2015.07.023>
- Yohandri Syafrindo, R. A., Sumantyo, J. T. S., Santosa, C. E., & Munir, A. (2017). 3D print X-band horn antenna for ground-based SAR application. *2017 Progress in Electromagnetics Research Symposium*. <https://doi.org/10.1109/PIERS.2017.8261940>
- Hatz, C. R., Msallem, B., Aghlmandi, S., Brantner, P., & Thieringer, F. M. (2020). Can an entry-level 3D printer create high-quality anatomical models? Accuracy assessment of mandibular models printed by a desktop 3D printer and a professional device. *International Journal of oral and maxillofacial surgery*, 49(1), 143–148. <https://doi.org/10.1016/j.ijom.2019.03.962>
- Dul, S., Fambri, L., & Pegoretti, A. (2016). Fused deposition modeling with ABS/graphene nanocomposites. *Applied Science and Manufacturing*, 85, 181–191. <https://doi.org/10.1016/j.compositesa.2016.03.013>
- Weng, Z., Wang, J., Senthil, T., & Wu, L. (2016). Mechanical and thermal properties of ABS/montmorillonite nanocomposites for fused deposition modeling 3D printing. *Materials & Design*, 102(15), 276–283. <https://doi.org/10.1016/j.matdes.2016.04.045>
- Park, S., Smallwood, A. M., & Ryu, C. Y. (2019). Mechanical and thermal properties of 3D-printed thermosets by stereolithography. *Journal of Photopolymer Science and Technology*, 32(2), 227–232. <https://doi.org/10.2494/photopolymer.32.227>
- Ikonomov, P. G., Yahamed, A., Fleming, P. D., & Pekarovicova, A. (2020). Design and testing 3D printed structures for bone replacements. *Journal of Achievements in Materials and Manufacturing Engineering*, 2(101), 76–85. <https://doi.org/10.5604/01.3001.0014.4922>
- You, D. H. (2016). Optimal printing conditions of PLA printing material for 3D printer. *The Transactions of the Korea Institute of Electrical Engineers*, 64(5), 825–830. <https://doi.org/10.5370/KIEE.2016.65.5.825>
- Choi, W., Woo, J. H., Jeon, J. B., & Yoon, S. S. (2015). Measurement of structural properties of PLA filament as a supplier of 3D printer. *Journal of the Korean Society of Agricultural Engineers*, 57(6), 141–152. <https://doi.org/10.5389/KSAE.2015.57.6.141>
- Perigaud, A., Bila, S., Tantot, O., Delhote, N., & Verdeyme, S. (2016). 3D printing of microwave passive components by different additive manufacturing technologies. *2016 IEEE MTT-S International Microwave Workshop Series on Advanced Materials and Processes for RF and THz Applications*. <https://doi.org/10.1109/IMWS-AMP.2016.7588328>
- Lawley, P. (2015). Applications of ultrasonic non-destructive testing in 3D printing. *The Journal of Undergraduate Research (SDSU)*, 13(4), 27–42.
- Elsaadouny, M., Barowski, J., & Rolfes, I. (2019). A convolutional neural network for the non-destructive testing of 3D-printed samples. *2019 44th International Conference on Infrared, Millimeter and Terahertz Waves*. <https://doi.org/10.1109/IRMMW-THz.2019.8874445>
- Elsaadouny, M., Barowski, J., Jebramcik, J., & Rolfes, I. (2019). Millimeter wave SAR imaging for the non-destructive testing of 3D-printed samples. *2019 44th International Conference on Electromagnetics in Advanced Applications*. <https://doi.org/10.1109/ICEAA.2019.8879272>
- Elsaadouny, M., Barowski, J., & Rolfes, I. (2019). Non-destructive testing of 3D-printed samples based on machine learning. *IEEE MTT-S, 2019*, 22–24. <https://doi.org/10.1109/IMWS-AMP.2019.8880141>
- Ma, C., Dong, Y., & Ye, C. (2016). Improving surface finish of 3D-printed metals by ultrasonic nanocrystal surface modification. *Procedia CIRP*, 45, 319–322. <https://doi.org/10.1016/j.procir.2016.02.339>
- Zhang, H., Chiang, R., Qin, H., Ren, Z., Hou, X., Lin, D., Doll, G. L., Vasudevan, V. L., Dong, Y., & Ye, C. (2017). The effects of ultrasonic nanocrystal surface modification on the fatigue performance of 3D-printed Ti64. *International Journal of Fatigue*, 103, 136–146. <https://doi.org/10.1016/j.ijfatigue.2017.05.019>
- Zhang, H., Zhao, J., Liu, J., Qin, H., Ren, Z., Doll, G. L., Dong, Y., & Ye, C. (2018). The effects of electrically-assisted ultrasonic nanocrystal surface modification on 3D-printed Ti-6Al-4V alloy. *Additive Manufacturing*, 22, 60–68. <https://doi.org/10.1016/j.addma.2018.04.035>
- Ko, S., & Lee, D. (2015). A study on cutting test and analysis of stiffness to various materials for developing complex 3D printing platform performing laminating and cutting. *70th Anniversary Conference of the KSME, 2015(11)*, 1901–1906.
- Caminero, M. A., Garcia-Moreno, I., Rodriguez, G. P., & Chacon, J. M. (2019). Internal damage evaluation of composite structures using phased array ultrasonic technique: Impact damage assessment in CFRP and 3D printed reinforced composites. *Composites, Part B: Engineering*, 165, 131–142. <https://doi.org/10.1016/j.compositesb.2018.11.091>

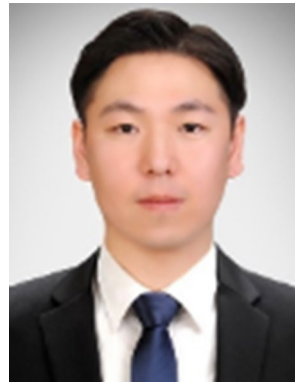
23. Cerniglia, D., Scafidi, M., Pantano, A., & Rudlin, J. (2015). Inspection of additive- manufactured layered components. *Ultrasonics*, 62, 292–298. <https://doi.org/10.1016/j.ultras.2015.06.001>
24. Choi, S., Park, J., & Lee, J. (2021). A study on the correlation between ultrasonic velocity and laminating thickness of 3D printed specimens. *Journal of the Korean Society for Nondestructive Testing*, 41(2), 102–109. <https://doi.org/10.7779/JKSNT.2021.41.2.102>
25. Lesseur, J., Tranchand, B., Mancier, T., Montauzier, A., Larignan, C., & Perusin, S. (2022). On the use of X-ray microtomography to control artificial defect geometries produced by metal additive manufacturing. *Nondestructive Testing and Evaluation*, 37(5), 611–630. <https://doi.org/10.1080/10589759.2022.2085701>
26. Song, J., Xu, C., & Li, Z. (2018). Ultrasonic nondestructive testing and regulation technology of residual stress. *Materials Science and Engineering*, 397, 012136. <https://doi.org/10.1088/1757-899X/397/1/012136>
27. Ke, Q., Li, W., Wang, W., & Song, S. (2022). Correction method with stress field effects in ultrasound nondestructive testing. *Non-destructive Testing and Evaluation*, 37(3), 277–296. <https://doi.org/10.1080/10589759.2021.1995384>
28. Li, W., Chen, B., Qing, X., & Cho, Y. (2019). Characterization of microstructural evolution by ultrasonic nonlinear parameters adjusted by attenuation factor. *Metals*, 9, 271. <https://doi.org/10.3390/met9030271>
29. Li, W., Jiang, C., & Deng, M. (2019). Thermal damage assessment of metallic plates using a nonlinear electromagnetic acoustic resonance technique. *NDT and E International*, 108, 102172. <https://doi.org/10.1016/j.ndteint.2019.102172>
30. Park, J., Lee, J., Min, J., & Cho, Y. (2020). Defects inspection in wires by nonlinear ultrasonic-guided wave generated by electromagnetic sensors. *Applied Sciences*, 10(13), 4479. <https://doi.org/10.3390/app10134479>
31. Park, J., Choi, J., & Lee, J. (2021). A feasibility study for a nonlinear guided wave mixing technique. *Applied Sciences*, 11(14), 6569. <https://doi.org/10.3390/app11146569>
32. Rose, J. L. (2014). *Ultrasonic waves in solid media* (pp. 54–57). Cambridge University Press. <https://doi.org/10.1017/CBO9781107273610>

Publisher's Note Springer Nature remains neutral with regard to jurisdictional claims in published maps and institutional affiliations.

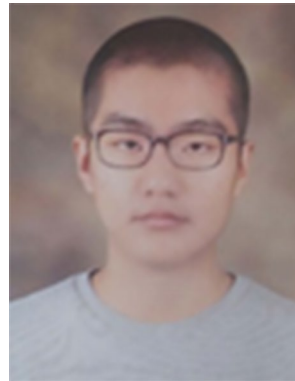
Springer Nature or its licensor (e.g. a society or other partner) holds exclusive rights to this article under a publishing agreement with the author(s) or other rightsholder(s); author self-archiving of the accepted manuscript version of this article is solely governed by the terms of such publishing agreement and applicable law.



Junpil Park is Postdoctoral Researcher of Extreme Environment Design and Manufacturing Innovation Center at Changwon National University. He received his Ph.D. from Pusan National University in 2019. His research interest are nondestructive testing, structural health monitoring, guided wave, tomography and nonlinear ultrasonic.



Sunho Choi received his Master degree from Changwon National University. His research interest is ultrasonic behavior of 3D products.



Seoung ho Baek is currently Researcher of Research Institute of Mechanical Technology at Pusan National University. His research topics are the design for additive manufacturing and process for reduce hydrogen embrittlement.



Sang hu Park is a Professor of Mechanical Engineering at Pusan National University. He earned his M.S. and Ph.D. in Mechanical Engineering at KAIST in 1996 and 2006, respectively. His research fields include engineering for additive manufacturing, sheet metal formation, and nanofabrication.



Yu-Hsi Huang is a Professor of Mechanical Engineering at National Taiwan University. He received his Ph.D. from National Taiwan University in 2009. His research fields are piezoelectric material and piezoelectricity, vibration, solid mechanics, and experimental mechanics.



Jaesun Lee is currently an Associate Professor of the Department of Mechanical Engineering at Changwon National University. He received his Ph.D. from Pusan National University in 2015. His main research interests are ultrasonic NDE/SHM, Long-range inspection, Theoretical wave scattering analysis and numerical simulation.